

THE SHAPE OF THE PRIMARY COSMIC RAY
ELECTRON SPECTRUM ABOVE 10 GeV

R. F. Silverberg, J. F. Ormes and V. K. Balasubrahmanyam

NASA/Goddard Space Flight Center

Greenbelt, Maryland (USA) 20771

A balloon borne measurement of the cosmic ray electron spectrum above 10 GeV is reported in which two new techniques have been used to remove proton background contamination. First, the depth of the spectrometer on one of the flights was more than 40 radiation lengths, the equivalent of more than 3 mean free paths of material, enabling hadronically and electromagnetically induced cascades to be differentiated for a subset of the data. Second, electromagnetic cascade starting points were determined to within about ± 0.1 radiation lengths based upon a calibration with electrons from 5.4 to 18 GeV at the Stanford Linear Accelerator, greatly reducing the chances for a proton to simulate an electron. The resulting spectrum, when fitted with a power law, is steep, -3.2 ± 0.1 , but the fit is marginal. A significantly better fit is achieved by assuming a model in which the spectrum is steepening in the measured region.

1. Introduction. While data on the energy spectrum of cosmic electrons up to several hundred GeV have been obtained in balloon flights, [Anand et al., 1969, Scheepmaker, 1971, Meyer and Muller, 1971], serious discrepancies in the spectral shape and absolute intensity are apparent. In the hope of clarifying the experimental situation, a large area detector was developed for use in a series of balloon flights. The experiment worked well on flights 1, 3 and 5. Flights 1 and 3 were flown from Alamogordo, New Mexico on April 28, 1969, at 7.9 g/cm^2 residual atmosphere and on November 11, 1970 at 7.4 g/cm^2 . The fifth flight was launched from Cape Girardeau, Missouri on October 1, 1972 and floated at 3.3 g/cm^2 . A total exposure factor of $\approx 7000 \text{ M}^2\text{-ster-sec}$ was obtained.

2. Description of the Detector. A diagram of the detector as flown on flight 3 is shown in figure 1. It consists of three sections: a section for particle identification, an electromagnetic shower section, and a nuclear cascade section. The charge module is made up of four detectors; two plastic scintillators, an acrylic plastic Cerenkov detector, and a cesium iodide scintillator. Each of these detectors is viewed by photomultipliers and their outputs are pulse height analyzed. Included in the charge module is a digital spark chamber which allows particle trajectories to be determined so that geometrical corrections can be made for the large area detectors.

The electromagnetic shower section is composed of twelve modules, each of which consists of a tungsten sheet and plastic scintillator representing

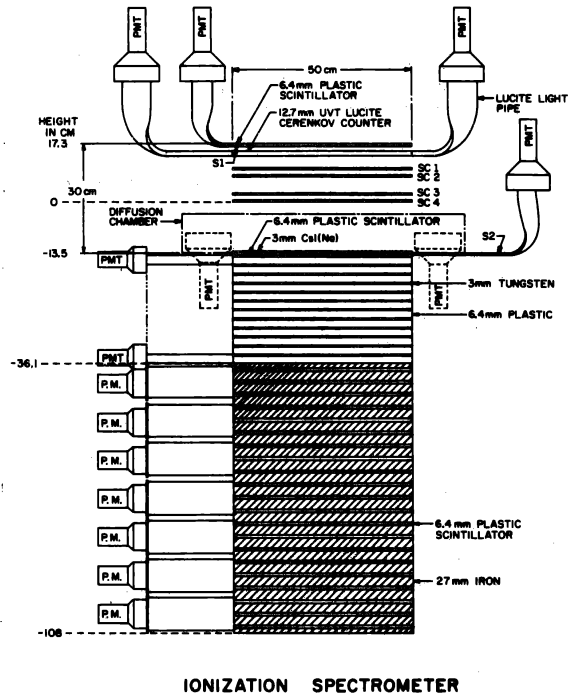
0.9 radiation lengths. Each module is viewed by two photomultiplier tubes whose outputs are summed and pulse height analyzed.

Although the nuclear cascade section was primarily for measurement of the high energy proton spectrum, it was extremely useful for determining the interacting proton background correction to the electron intensity. The nuclear cascade section consists of seven iron modules each one about 4.5 radiation lengths thick [0.5 nuclear mean free paths]. Each iron module is viewed by two photomultiplier tubes whose outputs are summed and pulse height analyzed.

The flight 1 configuration was the same as the flight 3 configuration except that the nuclear cascade section was not present. The flight 5 configuration is shown in figure 2. Flight 5 had an 18 module electromagnetic cascade section, and a time of flight detector to aid in background rejection. At this writing the processing of flight 5 data is incomplete so no spectrum for that flight can be given.

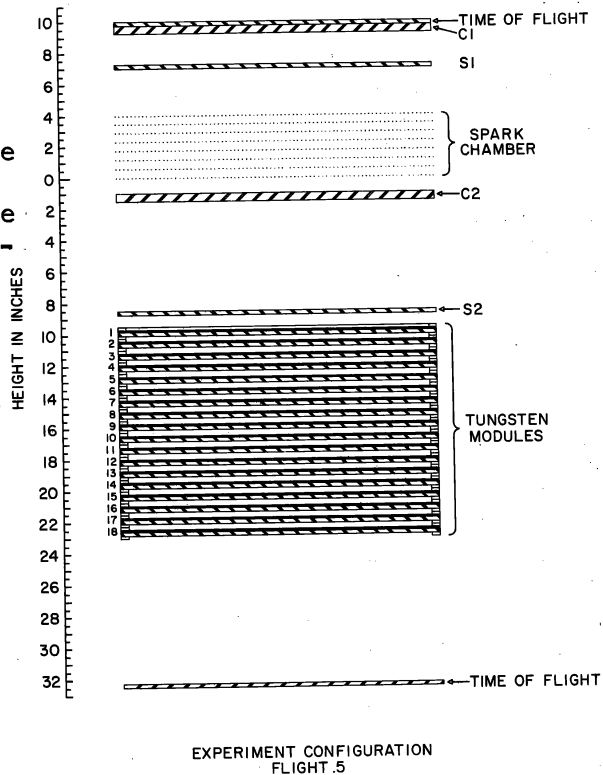
The instrument as shown in figure 1 was calibrated at the Stanford Linear Accelerator (SLAC) in 1969. The average shower profiles obtained from this calibration were extrapolated to higher energies using shower theory. A detailed description of the calibration procedure and the extrapolation of the calibration data will soon be published [Crannell et al., 1973].

3. Analysis of the Data. Since the electron component of cosmic rays is at best only a few percent of the proton component, the most serious problem in measuring electrons is to reduce to a negligible contribution those interacting protons which may masquerade as electrons. Our study of accelerator electrons and inflight high energy protons has revealed that the method of fitting the showers to equation 1



IONIZATION SPECTROMETER

Figure 1



EXPERIMENT CONFIGURATION
FLIGHT 5

Figure 2

below provides a sensitive means of discrimination against the proton background. In figure 3 a distribution of "apparent starting points" is presented for a sample of 16 GeV electrons from SLAC. This histogram is representative as no energy dependence was noted in the 5.4 to 18 GeV range. The distribution's width probably represents real fluctuations in the production of the first high energy cascade photon.

In contrast to the electrons, a group of singly charged particles was selected from the 1970 flight which deposited > 40 GeV in the iron and > 5 GeV in the tungsten. The condition that the energy deposited in the iron exceed the energy deposited in the tungsten was also imposed to get a set of inflight interacting protons. Their "apparent starting point" distribution is plotted in figure 4. The distribution in figure 4 exhibits marked structure. The source of the structure is not completely understood (See Crannell et al., 1973b for discussion). However, this difference limits the depth in which a proton can interact to simulate an electron.

Each possible event is examined to be sure that it is caused by a singly charged particle as determined by the top plastic scintillator and the Cerenkov detector. If the particle is singly charged, the spark chamber data is used to extrapolate the path of the particle to the twelfth tungsten module. Only particles whose trajectories pass within the inner 80% of the area of the 12th tungsten module are analyzed so edge effects are minimized. Each event accepted is then fitted to the electromagnetic shower function to determine its energy, E_0 , and apparent starting point, t_0 . This is done by minimizing the function

$$\chi^2 = \sum_{i=1}^{12} \left\{ \frac{f(E_0, t_0, t_i) - f_i}{\sigma(E_0, t_0, t_i)} \right\}^2 \quad (1)$$

where f_i is the observed energy deposition, $f(E_0, t_0, t_i)$ is the energy deposition caused by an electron of energy E_0 , at depth t_i if it started its cascade at depth t_0 , and $\sigma(E_0, t_0, t_i)$ is the expected standard deviation in $f(E_0, t_0, t_i)$. The minimum value of χ^2 (obtained by varying E_0 and t_0) is then

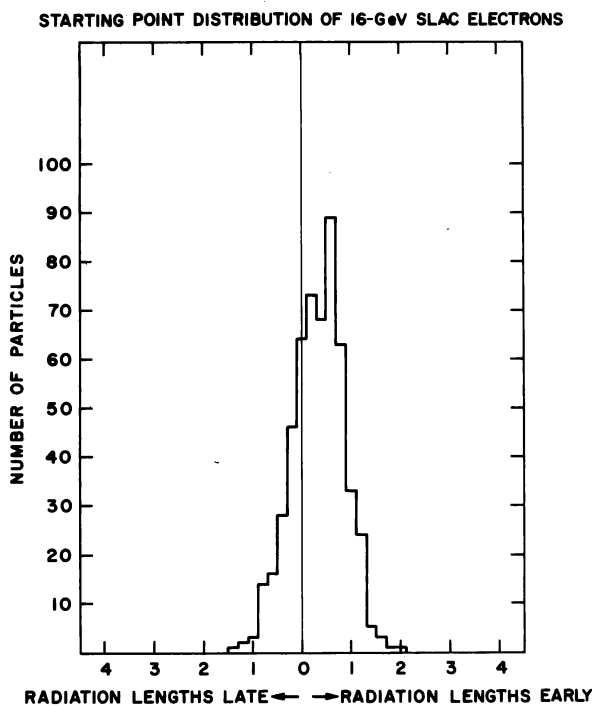


Figure 3

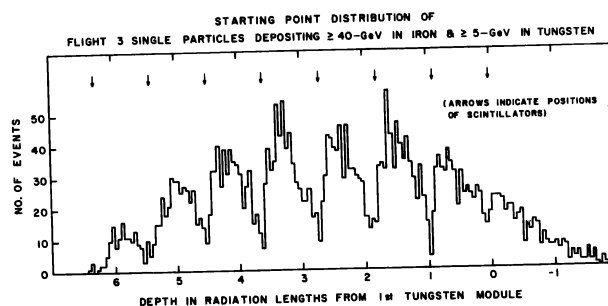


Figure 4

examined. If the minimum χ^2 for the event is below the value for 95% of the electrons of energy E_0 , and if the starting point is in the range for electrons observed at SLAC, the particle is accepted as an electron.

4. Residual Proton Background and Other Corrections. Even though unambiguous identification of each incident particle should be attainable with nuclear emulsions, emulsion techniques are responsible for perhaps the highest [Anand et al., 1968] and the lowest [Marar et al., 1971] measured primary cosmic ray electron intensities. Other workers have used statistical separation of the protons and electrons. Scheepmaker [1971] has used the spectrum of interacting alpha particles in flight to estimate the interacting proton spectrum. Earl et al., [1972] and Meyer and Müller, [1971] have used data and extrapolations from accelerator pions and protons to determine the proton induced contamination.

The unique feature of this experiment is its total depth of ~ 4 nuclear mean free paths of material. This depth allows secondaries from nuclear interactions to interact again and reveal themselves as proton induced showers. Thus while our rejection of such events is still a statistical one, we can use flight data itself to determine the proton background for this experiment. A subset of the apparent electrons [those which satisfied all of the above criteria] is selected which have trajectories which pass through at least three of the seven iron modules. This subset of about 25% of the events on flight 3 is examined to determine the fraction which deposited significantly more energy in the iron than could be expected of an electron of energy E . This leads to a $29 \pm 5\%$ correction which is then applied to all the data. The final correction for proton contamination as determined by the spectrometer is nearly energy dependent. This is surprising because of the difference in spectra. The proton rejection due to starting point and cascade shape is probably better at high energies because the electromagnetic showers are less subject to fluctuations than their hadronic counterparts. This shows the background rejection ratio is improving at the same time the proton to electron ratio is going up. On the other hand, we would like to point out that a proton contamination of only 30% at low energies could become much larger in other experiments at high energies since the electron and proton spectra are not the same.

The final spectrum includes corrections to the data for energy loss due to bremsstrahlung in the residual atmosphere, atmospheric secondaries, spark chamber inefficiency and dead time due to paralysis of the experiment during event readout. The correction for re-entrant albedo electrons is negligible at the energies measured.

Extensive investigations for any energy dependent effect in selection were also carried out. Energy dependence due to backscatter into the spark chamber or into the charge determination section was studied by examining the data from the spark chamber and the S_2 scintillator below it, as a function of energy. No significant correlation was found between large numbers of sparks and large pulse heights in the scintillator as a function of the energy of the incident particle. No determination of any backward transport of gamma rays could be made, but the work of Ford [1972] indicates that backscattering gamma rays greater than 2 MeV occur in less than 2% of the electron showers at high energies.

A significant energy dependence was found in the χ^2 distribution, an effect that was also observed in our SIAC data. The χ^2 value below which 95% of the SIAC positrons fell was found to increase like $E^{0.31}$. The spreading of the χ^2 distribution is qualitatively in agreement with our expectation since we observed that the standard deviations in the showers were larger than expected early in the showers. As energy rises there are more data points early in the shower [relative to shower maximum] and hence our underestimation of the deviations would make the parameter χ^2 rise as a function of energy.

To check further for energy dependent effects, the spectrum of singly charged particles that failed the electron test was found. This index was -2.7 ± 0.2 , the same as the high energy proton spectrum [Ryan et al., 1972].

5. Discussion. While the intensity in figure 5 agrees with the measurements of many other workers at about 10 GeV, the spectrum is significantly steeper. Assuming the data can be represented by a single power law over the range 10-200 GeV, the spectral index obtained is -3.2 ± 0.1 . This spectral index is steeper than the often quoted value of ~ -2.7 , [Bleeker, et al., 1968, Scheepmaker, 1971], although steep spectra have previously been reported [Earl et al., 1972, Webber and Rockstroh, 1973]. Our spectrum shows no sharp break but does exhibit a consistent drop off in intensity. The Chi-square test applied to the observed spectrum indicates that a power law represents only a marginal fit to the data (almost 3 standard deviations).

Due to the marginal fit of our data to a power law, a fit to the leakage lifetime model was attempted. From Cowsik et al., [1966], we find that with a source spectrum of the form $Q(E) \rightarrow E^{-\Gamma}$, the equilibrium intensity $I(E)$, would satisfy the expression

$$I(E)E^{\Gamma} \rightarrow \int_0^{1/\alpha} (1-\alpha x)^{\Gamma-2} e^{-x} dx \quad (2)$$

where $\alpha = \frac{WET}{307}$, W is the electromagnetic energy density in eV/cm^3 , T is the mean electron lifetime in mega-years and $\alpha=1$ is defined as the break energy. We call this the transition region model because the slope of the spectrum is changing. This model fits the data at about the 1 standard deviation level and yields -2.7 for Γ , and a break energy of ~ 50 GeV [lifetime $\sim 6 \times 10^6$ years assuming $W \sim 1 \text{ eV}/\text{cm}^3$]. Not too much significance can be attached to the particular model used or to the

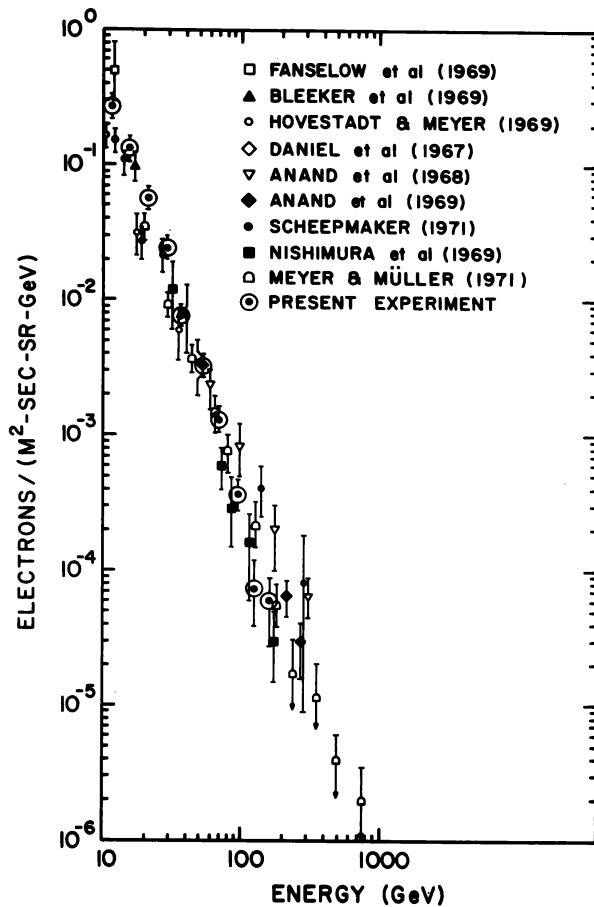


Figure 5

values obtained for the parameters; the transition region model contained one more free parameter than the power law model, and the minimum in the chi-square was very broad. The two fits to the data are illustrated in figure 6 where $E^3 \frac{dN}{dE}$ is plotted as a function of energy.

Our data thus argues strongly against a spectrum as hard as -2.7 around 100 GeV, and is suggestive that the data cannot be represented by a single power law over the range 10-200 GeV. The theoretical interpretation of this result in terms of the leakage lifetime approximation is not clear.

6. References. Anand, K. C., R. R. Daniel, and S. A. Stephens, Phys. Rev. Lett., 20, 764, 1968

Anand, K. C., R. R. Daniel, and S. A. Stephens, Paper OG-41, Proc. XIth Int. Conf. on Cosmic Rays, Budapest, 1969

Bleeker, J. A. M., J. J. Burger, A. J. M. Deerenberg, A. Scheepmaker, B. N. Swanenburg, and Y. Tanaka, Can. J. of Physics, 46, S522, 1968

Crannell, C. J., R. A. Gearhart, F. A. Hagen, W. V. Jones, R. J. Kurz, J. F. Ormes, R. D. Price, R. F. Silverberg, and G. M. Simnett, Nucl. Instr. and Methods, 1973, in press

Crannell, C. J., W. V. Jones, R. J. Kurz, R. F. Silverberg, W. Viehmann, to be published in Proc. of XIIIth Int. Conf. on Cosmic Rays, 1973b.

Cowsik, R., Y. Pal, S. N. Tandon, and R. P. Verma, Phys. Rev. Lett., 17, 1298, 1966

Daniel, R. R., and S. A. Stephens, Proc. Ind. Acad. Sci., 65, 319, 1967

Earl, J. A., D. E. Neally, and T. A. Rygg, J. Geophys. Res. 77, 1087, 1972

Fanselow, J. L., R. C. Hartman, R. H. Hildebrand and P. Meyer, Astrophys. J., 158, 771, 1969

Ford, R., Private Communication, 1972

Hovestadt, D., and P. Meyer, Paper MO-118, Proc: XIth Int. Conf. on Cosmic Rays, Budapest, 1969

Marar, T. M. K., P. S. Frier and C. J. Waddington, J. Geophys. Res., 76, 1625, 1971

Meyer, P. and D. Müller, Paper OG-36, Proc. XIIth Int. Conf. on Cosmic Rays, Hobart, Tasmania, 1971

Nishimura, J., E. Mikumo, I. Mito, K. Niu, I. Ohto, and I. Tiara, Paper OG-43 Proc. XIth Int. Conf. on Cosmic Rays, Budapest, 1969

Ryan, M. J., J. F. Ormes, and V. K. Balasubrahmanyam, Phys. Rev. Lett., 28, 985, 1972

Scheepmaker, A., unpublished thesis, U. of Leiden, 1971

Webber, W. R. and J. M. Rockstroh, J. Geophys. Res., 78, 1, 1973

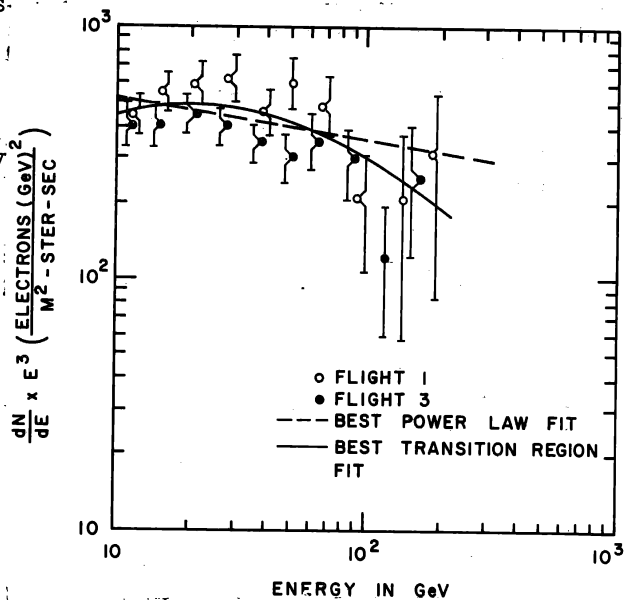


Figure 6